DISCRETIZATION OF DYNAMIC LOADING IN TIME HISTORY ANALYSIS

S.-Y. Chang *

Department of Civil Engineering
National Taipei University of Technology
Taipei, Taiwan 10608, R.O.C.

ABSTRACT

Although the numerical properties of a step-by-step integration method can be evaluated based on the currently available techniques, there is still lack of a technique for evaluating its capability to capture dynamic loading. In this work, the amplitude error caused by the step discretization error is identified and the correlation between the relative amplitude error and relative step discretization error is analytically established. As a result, it is thoroughly confirmed that the asymptotic constant of the discretization error amplification factor for the displacement response to a cosine loading can be considered as an indicator of the capability to capture dynamic loading for a general step-by-step integration method.

Keywords: Equations of motion, Dynamic loads, Dynamic analysis, Solutions, Accuracy.

1. INTRODUCTION

The step-by-step integration method (Newmark [1]; Hilber *et al.* [2]; Chang [3-5]) might be the most powerful technique for nonlinear dynamic analysis. Stability, convergence and accuracy are the three important requirements for an integration method (Belytschko and Hughes [6]). Accuracy implies that an integration method should give a result close enough to the exact solution. This is because that any integration method can only give an approximate solution to the equations of motion due to simplifying assumptions used in the integration procedure. In general, numerical errors will be introduced due to the use of difference equations, inaccurate representation of dynamic loading and the assumption that structural properties remain unchanged within a time step. The numerical properties of an integration method regarding numerical accuracy have been explored. However, it seems that all the evaluation techniques for numerical accuracy are based on the free vibration response and the influence of dynamic loading force is neglected.

Since the dynamic loading usually has a major effect on a solution of the equation of motion, it is of need to capture it properly so that a reliable solution can be obtained. However, there is still lack of an evaluation technique that can be used to determine if the dynamic loading is accurately captured. Hence, it is needed to study the capability in capturing dynamic loading for an integration method. To develop a technique for this purpose, the accuracy of the displacement responses to some analytical loading types for a single degree of freedom system is evaluated by comparing numerical solutions to exact solutions, which are theoretically obtained. In this work, two schemes are applied to yield the displacement responses. One is to use a spectral decomposition technique to obtain the displacement responses from the Newmark family method and the other is obtained from the fundamental theory of the structural dynamics. After comparing the numerical solutions to exact solutions, numerical accuracy of the displacement response to a dynamic loading can be evaluated.

2. THEORETICAL DISPLACEMENT RESPONSES

In structural dynamics, the equation of motion for a single degree of freedom system can be expressed as

$$m\ddot{u} + c\dot{u} + ku = f \tag{1}$$

where u, $\dot{u}$ and $\ddot{u}$ are the displacement, velocity and acceleration, respectively. In general, a closed-form solution of this equation can be obtained if f consists of simple analytical functions. Hence, some specific loading types are considered and expressed as

$$\begin{aligned} f(t) &= a + b\left(\frac{t}{t_d}\right) + c\left(\frac{t}{t_d}\right)^2 && \text{(Polynomial Loading)} \\ f(t) &= a\sin\left(\frac{2\pi t}{t_d}\right) && \text{(Sine Loading)} \\ f(t) &= a\cos\left(\frac{2\pi t}{t_d}\right) && \text{(Cosine Loading)} \end{aligned} \tag{2}$$

* Corresponding author (changsy@ntut.edu.tw)

DOI : 10.1017/jmech.2013.68
Copyright © 2014 The Society of Theoretical and Applied Mechanics, R.O.C.
https://doi.org/10.1017/jmech.2013.68 Published online by Cambridge University Press

where $t \le t_d$ and t_d is the loading duration; a, b and c are constants. Both theoretical and numerical solutions of Eq. (1) subject to these three dynamic loadings will be obtained so that the numerical accuracy of the displacement response to each dynamic loading can be evaluated. The choices of the three dynamic loading types are due to the fact that (a) a recorded ground motion is generally made up of a series of zigzag dynamic loadings, which is a special case of the polynomial loading if choosing $c = 0$; (b) any dynamic loading can be considered as a combination of sine and cosine loadings based on the concept of Fourier series. Thus, the results may be applied to a general dynamic loading except for load discontinuity (Chang [7]).

Apparently, closed-form solutions to the three dynamic loadings with the initial conditions of d_0 and v_0 can be obtained (Chopra [8]). If the loading duration is equally subdivided into p time steps and the step size is taken as Δt, after substituting $t_d = p(\Delta t)$ and $t = (n + 1)(\Delta t)$ into the theoretical solutions, the discrete displacements at the $(n + 1)$-*th* time step are found to be

$$
\begin{aligned}
d_{n+1} &= \sqrt{\left[d_0 - \frac{a}{k} + \frac{c}{k}\frac{2}{(p\Omega)^2}\right]^2 + \frac{1}{\Omega^2}\left[(\Delta t)v_0 - \frac{b}{k}\frac{1}{p}\right]^2}\,\sin\left[(n+1)\Omega + \theta\right] \\
&\quad + \frac{c}{k}\left(\frac{n+1}{p}\right)^2 + \frac{b}{k}\frac{n+1}{p} + \frac{a}{k} - \frac{c}{k}\frac{2}{(p\Omega)^2} \\
d_{n+1} &= \frac{1}{\Omega}\left\{(\Delta t)v_0 - \left(\frac{a}{k}\right)\left[\frac{\frac{2\pi}{p}}{1-\left(\frac{2\pi}{p\Omega}\right)^2}\right]\right\}\sin(n+1)\Omega \\
&\quad + \left(\frac{a}{k}\right)\left[\frac{1}{1-\left(\frac{2\pi}{p\Omega}\right)^2}\right]\sin\frac{(n+1)2\pi}{p} \\
d_{n+1} &= \left\{d_0 - \left(\frac{a}{k}\right)\left[\frac{1}{1-\left(\frac{2\pi}{p\Omega}\right)^2}\right]\right\}\cos(n+1)\Omega \\
&\quad + \left(\frac{a}{k}\right)\left[\frac{1}{1-\left(\frac{2\pi}{p\Omega}\right)^2}\right]\cos\frac{(n+1)2\pi}{p}
\end{aligned}
\tag{3}
$$

for the three dynamic loadings, where $\Omega = \omega(\Delta t)$ and $\omega = \sqrt{k/m}$ is the natural frequency of the system. In addition, $\theta = \left[d_0 - \frac{a}{k} + \frac{c}{k}\frac{2}{(p\Omega)^2}\right] / \left[\frac{(\Delta t)v_0}{\Omega} - \frac{b}{k}\frac{1}{p\Omega}\right]$ is defined. Since $t \le t_d$ is assumed in the derivations $(n + 1) \le p$ must be satisfied.

3. NUMERICAL DISPLACEMENT RESPONSES

Many integration methods can be used to solve Eq. (1). In this study, the Newmark family method is considered and it can be expressed as

$$
\begin{aligned}
& ma_{n+1} + cv_{n+1} + kd_{n+1} = f_{n+1} \\
& d_{n+1} = d_n + (\Delta t)v_n + (\Delta t)^2\left[\left(\frac{1}{2} - \beta\right)a_n + \beta a_{n+1}\right] \\
& v_{n+1} = v_n + (\Delta t)\left[(1-\gamma)a_n + \gamma a_{n+1}\right]
\end{aligned}
\tag{4}
$$

where d_n, v_n and a_n are approximations to $u(t_n)$, $\dot{u}(t_n)$ and $\ddot{u}(t_n)$ at the n-*th* time step. Since $\gamma = 1/2$ is necessary for the Newmark family method to at least have an accuracy of second order, the subfamily of $\gamma = 1/2$ is studied. There are four well-known members of this subfamily. They are the Newmark explicit method (NEM, $\beta = 0$), the Fox-Goodwin method (FGM, $\beta = 1/12$), the linear acceleration method (LAM, $\beta = 1/6$) and the constant average acceleration method (AAM, $\beta = 1/4$). In general, they have an order of accuracy 2 except that the Fox-Goodwin method is third-order accurate (Belytschko and Hughes [6]; Bathe [9]).

Numerical solutions will be obtained by spectral decomposition (Belytschko and Hughes [6]; Strang [10]). For this purpose, the subfamily of the Newmark family method can be rewritten in a recursive matrix form as

$$
\mathbf{X}_{n+1} = \mathbf{A}\mathbf{X}_n + \mathbf{L}f_{n+1} = \mathbf{A}^{n+1}\mathbf{X}_0 + \sum_{i=0}^{n}\mathbf{A}^{(n-i)}\mathbf{L}f_{i+1} \tag{5}
$$

where $\mathbf{X}_n = [d_n,\ (\Delta t)v_n,\ (\Delta t)^2 a_n]^{\mathrm{T}}$ and $\mathbf{X}_0 = [d_0,\ (\Delta t)v_0,\ \Omega^2(f_0/k - d_0)]^{\mathrm{T}}$. A pair of complex conjugate eigenvalues in addition to a zero eigenvalue can be found from $(\mathbf{A} - \lambda\mathbf{I})\,\mathbf{X} = 0$ and are

$$
\lambda_{1,2} = e^{-\bar{\xi}\bar{\Omega} \pm j\bar{\Omega}} = e^{-\bar{\xi}\bar{\Omega}}(\cos\bar{\Omega} \pm j\sin\bar{\Omega}) \tag{6}
$$

where $e^{-\bar{\xi}\bar{\Omega}} = 1$, $\cos\bar{\Omega} = \left[1 + \left(\beta - \frac{1}{2}\right)\Omega^2\right] / (1 + \beta\Omega^2)$ and $\sin\bar{\Omega} = \left[\Omega\sqrt{1 + \left(\beta - \frac{1}{4}\right)\Omega^2}\right] / (1 + \beta\Omega^2)$; $\bar{\xi}$ is a numerical damping ratio and $\bar{\Omega} = \bar{\omega}(\Delta t)$; $\bar{\Omega}$ and $\bar{\omega}$ are often considered as the quantities corresponding to Ω and ω in a numerical solution. There is no numerical dissipation for this subfamily of integration methods since $\bar{\xi} = 0$ is indicated by $e^{-\bar{\xi}\bar{\Omega}} = 1$.

After spectral decomposition and algebraic manipulations, the discrete solutions to the three dynamic loadings at the $(n + 1)$-*th* step as $(i + 1) \le p$ for using the subfamily of the Newmark method are found to be

https://doi.org/10.1017/jmech.2013.68 Published online by Cambridge University Press

$$d_{n+1}=\sqrt{\left[d_0-\frac{a}{k}+\frac{c}{k}\frac{2}{(p\Omega)^2}\right]^2+\left(\frac{2\sin\frac{1}{2}\bar{\Omega}}{\Omega^2\cos\frac{1}{2}\bar{\Omega}}\right)^2\left[(\Delta t)v_0-\frac{b}{k}\frac{1}{p}\right]^2}\sin\left[(n+1)\bar{\Omega}+\bar{\theta}\right]$$
$$+\frac{c}{k}\left(\frac{n+1}{p}\right)^2+\frac{b}{k}\frac{n+1}{p}+\frac{a}{k}-\frac{c}{k}\frac{2}{(p\Omega)^2}$$

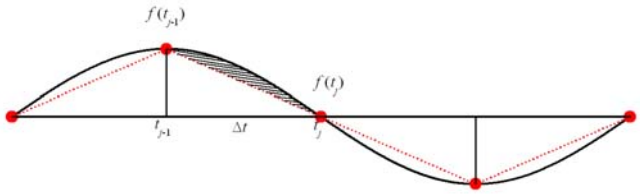
$$d_{n+1}=\frac{1}{\Omega}\left\{(\Delta t)v_0-\left(\frac{a}{k}\right)\left(\frac{2\sin\frac{1}{2}\bar{\Omega}}{\Omega\cos\frac{1}{2}\bar{\Omega}}\right)\frac{\sin\left(\frac{2\pi}{p}\right)}{1-\left[\frac{\sin(\pi/p)}{\sin(\bar{\Omega}/2)}\right]^2}\right\}\sin(n+1)\bar{\Omega}+\left(\frac{a}{k}\right)\left\{\frac{1-4\beta\sin^2\left(\frac{\pi}{p}\right)}{1-\left[\frac{\sin(\pi/p)}{\sin(\bar{\Omega}/2)}\right]^2}\right\}\sin\frac{(n+1)2\pi}{p}$$

$$d_{n+1}=\left\{d_0-\left(\frac{a}{k}\right)\frac{1-4\beta\sin^2\left(\frac{\pi}{p}\right)}{1-\left[\frac{\sin(\pi/p)}{\sin(\bar{\Omega}/2)}\right]^2}\right\}\cos(n+1)\bar{\Omega}+\left(\frac{a}{k}\right)\left\{\frac{1-4\beta\sin^2\left(\frac{\pi}{p}\right)}{1-\left[\frac{\sin(\pi/p)}{\sin(\bar{\Omega}/2)}\right]^2}\right\}\cos\frac{(n+1)2\pi}{p} \tag{7}$$

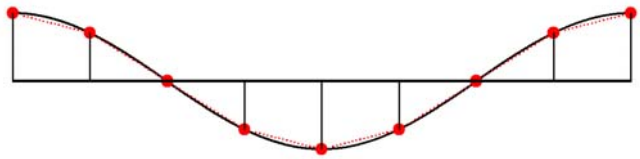
where $\theta=\left[d_0-\frac{a}{k}+\frac{c}{k}\frac{2}{(p\Omega)^2}\right]\Big/\left[\left(\frac{2\sin\frac{1}{2}\bar{\Omega}}{\Omega^2\cos\frac{1}{2}\bar{\Omega}}\right)\left((\Delta t)v_0-\frac{b}{k}\frac{1}{p}\right)\right]$. The first term on the right hand side of the first line is the transient response while the rest terms are the steady-state responses. Meanwhile, the first term on the right hand side of the second and third lines is the transient response and the other term is the steady-state response.

4. DISCRETIZATION OF DYNAMIC LOAING

Any discretization error in the dynamic loading will result in a displacement response error. A discretization error is due to the use of a finite number of integration points to represent an analytical function. This case is schematically shown in Fig. 1, where a sine loading is captured by 4 integration time steps and a cosine loading is captured by 8 integration time steps. In this figure, a sine loading and a cosine loading, which are in an analytical form, are discretized so that they can match the input for the step-by-step integration. Thus, the shaded area as shown in Fig. 1(a) is the discretization error occurred within the *j-th* time step. This step error can be computed by using the following procedure.



(a) 4 integration time steps to capture sine loading



(b) 8 integration time steps to capture sine loading

Fig. 1 Discretization of dynamic loading

$$A_j^{(exa)}=\left|\int_{t_{j-1}}^{t_j} f(t)\,dt\right| \quad and \quad A_j^{(app)}=\left|\frac{f(t_{j-1})+f(t_j)}{2}(\Delta t)\right| \tag{8}$$

where $A_j^{(exa)}$ is the area enclosed by the solid line and the time-axis at the *j-th* time step and is an exact input area while $A_j^{(app)}$ is the area enclosed by the dotted line and the time-axis and is an approximation to the exact area. Apparently, the difference between the areas of $A_j^{(exa)}$ and $A_j^{(app)}$ is the step discretization error at the *j-th* time step. Thus, the relative step discretization error for this time step can be defined as

$$E_j=\frac{A_j^{(app)}-A_j^{(exa)}}{A_j^{(exa)}} \tag{9}$$

Thus, if t_d for the three dynamic loadings, as shown in Eq. (2), is equally subdivided into p time steps, E_j for each dynamic loading can be evaluated and is summarized in Table 1. In addition, the variation of E_j with p is plotted Fig. 2.

In the second column of Table 1, there will be no step discretization error for the polynomial loading if $c = 0$ in addition to any values of a and b, while E_j is constant if $a = b = 0$ for a given j. This constant drastically decreases from $j = 1$ to $j = 2$; subsequently it decreases step by step as j increases and finally tends to zero as p and j are large enough. This is manifested from Fig. 2. On the other hand, for the sine loading and cosine loading, the absolute value of the relative step discretization error decreases with the increase of the number of time steps. In addition, it will be reduced to zero for a large enough p value.

https://doi.org/10.1017/jmech.2013.68 Published online by Cambridge University Press

Table 1 Relative step discretization error

Loading Type	Polynomial Loading	Sine Loading	Cosine Loading
E_j	$\dfrac{a+\dfrac{\left(j-\frac{1}{2}\right)}{p}b+\dfrac{\left(j^2-j+\frac{1}{2}\right)}{p^2}c}{a+\dfrac{\left(j-\frac{1}{2}\right)}{p}b+\dfrac{\left(j^2-j+\frac{1}{3}\right)}{p^2}c}-1$	$\dfrac{\frac{\pi}{p}\cos\frac{\pi}{p}}{\sin\frac{\pi}{p}}-1$	$\dfrac{\frac{\pi}{p}\cos\frac{\pi}{p}}{\sin\frac{\pi}{p}}-1$

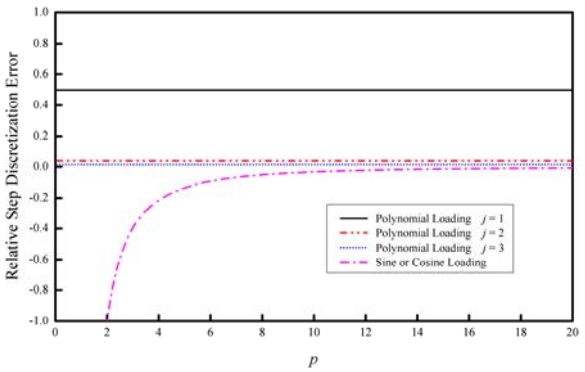


Fig. 2 Variation of relative step discretization error with p

5. AMPLITUDE DISTORTION

Period and amplitude distortions are usually found in a numerical solution, and thus are best suited to evaluating the numerical accuracy of the response. Both the theoretical and numerical solutions as shown in Eqs. (3) and (7) reveal that the state-state response is closely related to the dynamic loading and the value of Ω while the transient response only depends upon the value of Ω. Hence, if the dynamic loading is not realistically captured in the step-by-step integration procedure, numerical errors will be found in the total response.

Since period distortion in the transient response has been well studied (Belytschko and Hughes [6]) and there is no period distortion found in the steady-state response for the three dynamic loadings, only the amplitude distortion is addressed. It is appropriate to define the relative amplitude error, which is similar to the relative period error, so that amplitude distortion can be assessed. As a result, it is defined as

$$E_{amp}=\frac{\bar{A}-A}{A} \tag{10}$$

where $\bar{A}$ is the amplitude of the numerical solution and A is that of the theoretical solution. A positive relative amplitude error implies amplitude growth while amplitude decay is indicated by a negative value. The symbol of $E_{amp}^{(tra)}$ is the relative amplitude error for the transient response while $E_{amp}^{(ste)}$ is that for the steady-state response.

6. DISCRETIZATION ERROR AMPLIFICATION FACTOR

It is anticipated that the maximum displacement amplitude error will be closely correlated to the relative step discretization error of the dynamic loading for a step-by-step integration method. Thus, it is very straightforward to define a discretization error amplification factor, which is the ratio of the relative amplitude error, as shown in Eq. (10), over its corresponding relative step discretization error, as given in Eq. (9). Consequently, it can be expressed as

$$A_{tra}=\frac{E_{amp}^{(tra)}}{E_j} \quad \text{and} \quad A_{ste}=\frac{E_{amp}^{(ste)}}{E_j} \tag{11}$$

where A_{tra} is the discretization error amplification factor for the transient response, while that for the steady-state response is denoted by A_{ste}. These two discretization error amplification factors can be used to evaluate the numerical properties of a step-by-step integration method regarding to the maximum displacement amplitude error, which arises from the step discretization error of a dynamic loading.

7. COMPARISONS OF THEORETICAL AND NUMERICAL SOLUTIONS

After obtaining the theoretical and numerical solutions for a single degree of freedom system subject to the three dynamic loadings, and the introduction of the relative amplitude error and the discretization error amplification factors, the numerical properties of the subfamily of the Newmark method in capturing the dynamic loadings can be thoroughly discussed next.

7.1 Polynomial Loading

After comparing the first line of Eq. (7) to the first line of Eq. (3), it is found that the steady-state response to the specified polynomial loading is perfectly obtained for any member of the subfamily of the Newmark family method. However, errors are generally introduced in period and amplitude for the transient response. The period is generally distorted from Ω to $\bar{\Omega}$ for the transient response. To gain an insight into

https://doi.org/10.1017/jmech.2013.68 Published online by Cambridge University Press

the amplitude distortion of the transient response, the variation of $E_{amp}^{(tra)}$ with $p\Omega$ is shown in Fig. 3 and its corresponding A_{tra} with $p\Omega$ is plotted in Fig. 4. It is worth noting that the case of $a = c = 0$ and $b \neq 0$ is considered because this case will lead to a very significant period distortion. Since the loading duration t_d is equally subdivided into p time steps, a large value of p will lead to a small value of Ω. Hence, it is appropriate to plot the relative amplitude error with $p\Omega = \omega t_d$. This is because that only the small values of Ω are of interest for a large value of p.

In Fig. 3, the relative amplitude error increases with the increase of $p\Omega$ for NEM, FGM and LAM while it is always equal to 0 for AAM. In general, for a small value of $p\Omega$, the relative amplitude error is close to zero for the four methods. Thus, they have roughly the same capability to capture the polynomial loading. In each plot of Fig. 4, the discretization error amplification factor starts from the origin and then increases gradually for each curve except that it is always equal to 0 for AAM. The four curves are almost overlapped together in each plot. This implies that the relative step discretization error is amplified by roughly the same factor for a given $p\Omega$ and thus a large time step will lead to a large relative amplitude error since a large time step generally has a relatively large relative step discretization error for a given $p\Omega$ as shown in Fig. 3 except for Fig. 3(d).

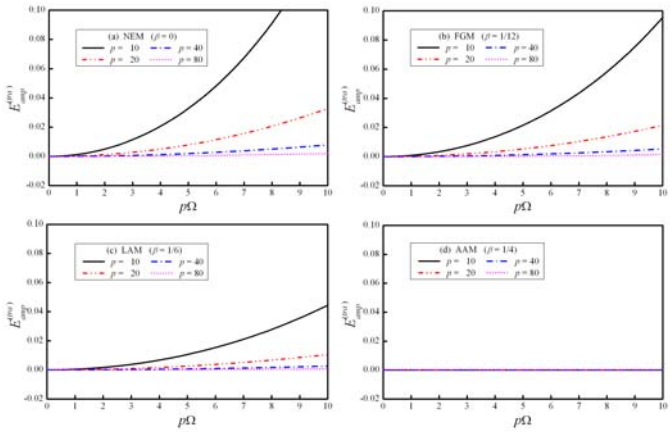


Fig. 3 Relative amplitude error of response to polynomial loading

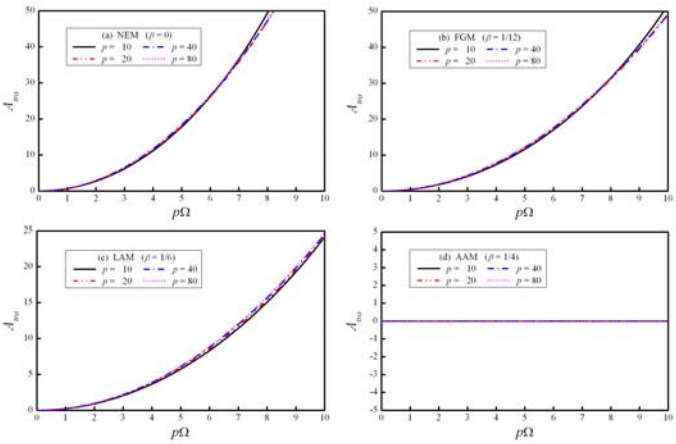


Fig. 4 Discretization error amplification factor for polynomial loading

7.2 Sine Loading

Comparing the second line of Eq. (3) to that of Eq. (7), the differences between the theoretical and numerical solutions for a sine loading can be evaluated. Both period and amplitude are distorted in the transient response, while there is only amplitude distortion in the steady-state response. The variations of amplitude distortion with $p\Omega$ for the transient response are plotted in Fig. 5 while those for the steady-state response are shown in Fig. 6.

Amplitude decay is generally found in each plot of Fig. 5 except that in Figs. 5(a) and 5(b) amplitude growth is found as $p\Omega$ is greater than a certain value, such as the value about 3.64 in Fig. 5(a) and the value between 5 and 6 in Fig. 5(b). On the other hand, amplitude growth is found in Figs. 6(a) and 6(b) while amplitude decay is found in Figs. 6(c) and 6(d). In general, amplitude distortion decreases with the increase of p for a given $p\Omega$ for the transient and steady-state responses. The relative amplitude error does not tend to zero as $p\Omega$ approaches zero except for a large p value. This implies that the p value must be chosen to be large enough so that the sine loading can be faithfully captured or amplitude distortion will occur even if $p\Omega$ is very small. After the comparisons of the four plots of Fig. 5, amplitude distortion in the transient response is roughly the same for all the four methods for a small $p\Omega$. However, in the steady-state response, AAM shows the largest amplitude distortion among the four methods for a small $p\Omega$; NEM and LAM have the

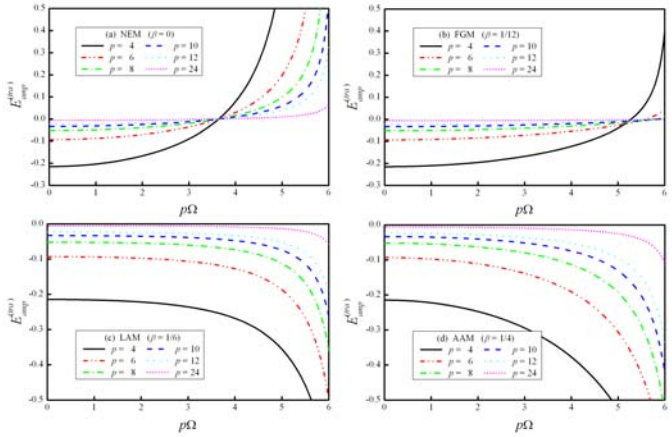


Fig. 5 Relative amplitude error for sine term of transient response to sine loading

moderate amplitude distortion and FGM shows the smallest amplitude distortion. Comparing Figs. 5 to 6, it is found that amplitude distortion in the transient response is roughly the same as that in the steady-state response for NEM and LAM, while that in the transient response is larger than that in the steady-state response for FGM and that in the transient response is less than that in the steady-state response for AAM.

https://doi.org/10.1017/jmech.2013.68 Published online by Cambridge University Press

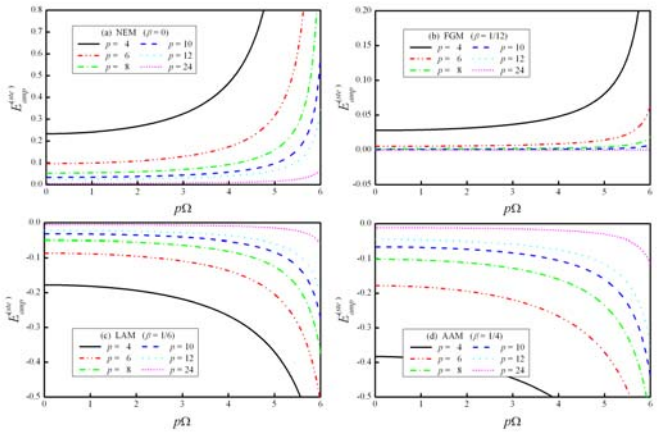


Fig. 6 Relative amplitude error of steady-state response to sine loading

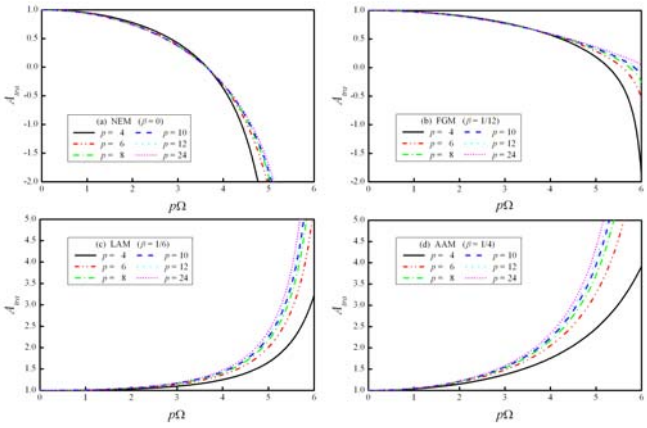


Fig. 7 Discretization error amplification factor for sine term of transient response to sine loading

The variations of the discretization error amplification factors for A_{tra} with $p\Omega$ are plotted in Fig. 7 while those for A_{ste} are shown in Fig. 8. Figure 7 shows that A_{tra} starts from 1 for each method and then decreases gradually with increasing $p\Omega$ for NEM and FGM while for LAM and AAM it increases gradually with the increase of $p\Omega$. It is also found that the four curves are almost clustered together for a small $p\Omega$ in each plot. In each plot Fig. 8, each curve of the discretization error amplification factor no longer starts from 1 for the four methods. However, these curves in each plot seem to converge to the curve which corresponds to a large enough p value. Furthermore, the converged starting value of each plot of this figure are found to be –1, 0 1 and 2 in correspondence to NEM, FGM, LAM and AAM as the value of p is large enough.

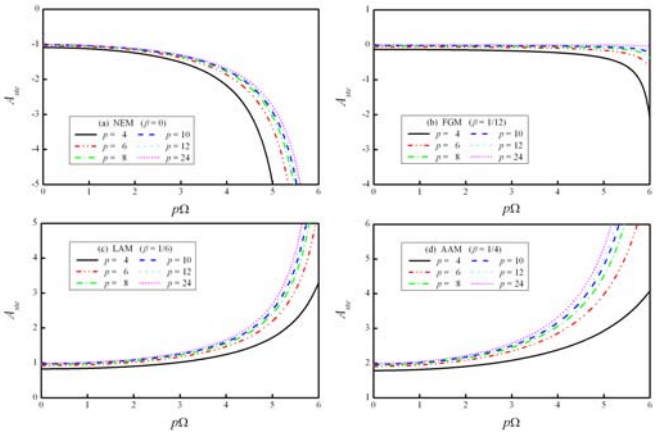


Fig. 8 Discretization error amplification factor of steady-state response to sine loading

7.3 Cosine Loading

Comparing the second line to the third line in Eq. (3), it is found that the absolute values of the coefficients for both the transient response and the steady-state response in the third line are exactly the same as that of the steady-state response in the second line. This relation is also found in the numerical solution of Eq. (7). This implies that amplitude distortion in the steady-state response and the transient response to the cosine loading is exactly the same as that in the steady-state response to the sine loading. Thus, the variations of the relative amplitude errors $E_{amp}^{(tra)}$ and $E_{amp}^{(ste)}$ with $p\Omega$, and their corresponding discretization error amplification factors for the cosine loading for each method are the same as those shown in Figs. 6 and 8, respectively. Hence, there is no need to plot these results again.

8. CAPABILITY IN CAPTURING DYNAMIC LOADING

In each plot of Fig. 4, A_{tra} starts from the origin in each curve for the transient response as a single degree of freedom system is subjected to a polynomial loading. A very similar phenomenon is also found in Fig. 7 for the transient response as the same system is excited by a sine loading, except that A_{tra} starts from 1 in each curve. In Fig. 8, it is found that A_{ste} no longer starts from the same value of 0 or 1 as $p\Omega \to 0$ and $p \to \infty$ in each curve as the system is subjected to a sine loading. The starting value varies not only with p but also the method used in Fig. 8. Although the starting value of each curve is different in each plot a certain asymptotic constant is converged for a specific method as the value of p is large enough.

It is of great interest to mathematically derive the asymptotic constants of the discretization error amplification factors for the four methods so that the results shown in Figs. 4, 7 and 8 can be confirmed. The asymptotic constants for the three dynamic loadings can be obtained by evaluating the limiting values of the discretization error amplification factors. The results loadings are listed in Table 2. The limiting values are achieved by expressing the harmonic functions as infinites series and then evaluating the limits. The results shown in Figs. 4, 7 and 8 are highly consistent with the asymptotic constants shown in Table 2.

In Fig. 4, the asymptotic constant is 0 for the four methods. This implies that the relative amplitude

https://doi.org/10.1017/jmech.2013.68 Published online by Cambridge University Press

Table 2 Asymptotic constants of discretization error amplification factors

Loading Type	Polynomial Loading	Sine Loading	Cosine Loading
$\lim_{p\Omega\to 0} A_{tra}^{(\sin)}$	0	1	N.A.
$\lim_{p\Omega\to 0} A_{tra}^{(\cos)}$	N.A.	N.A.	$12\left(\beta-\frac{1}{12}\right)$
$\lim_{p\Omega\to 0} A_{ste}$	0	$12\left(\beta-\frac{1}{12}\right)$	$12\left(\beta-\frac{1}{12}\right)$

error in the transient response to the polynomial loading tends to zero as $p\Omega \to 0$ for the four methods. Thus, the capability to capture the polynomial loading is roughly the same for small $p\Omega$ for the four methods. On the other hand, an asymptotic constant of 1 is found for the four methods in Fig. 7. It is indicated that the relative amplitude error for the transient response to the sine loading is equal to the step discretization error as $p\Omega \to 0$ for the four methods. In Fig. 8, different asymptotic constants are found for the four methods and they are 0, 1, –1 and 2 in correspondence to FGM, LAM, NEM and AAM. This reveals that the relative amplitude errors for the steady-state response to the sine loading are different for small $p\Omega$ for the four methods. In fact, for a small value of $p\Omega$, the relative amplitude error is roughly equal to the step discretization error for LAM and NEM, while it is about 2 times of the step discretization error for AAM and it will reduce to be smaller than the step discretization error for FGM.

In general, a step discretization error will lead to amplitude distortion and it seems appropriate to consider the asymptotic constant of the discretization error amplification factor as an indicator of the capability to capture dynamic loading for a step-by-step integration method since it is closely correlated to the step discretization error. In fact, the asymptotic constant of the discretization error amplification factor for a specific response to a given dynamic loading represents the amplification factor of the relative step discretization error as $p\Omega$ tends to zero and p is large enough. Hence, a large asymptotic constant implies a large amplitude distortion.

9. NUMERICAL CONFIRMATIONS OF ANALYTICAL RESULTS

In order to confirm the analytical results, some numerical examples are examined next. For this purpose, a single degree of freedom system subject to a polynomial loading, a sine loading and a cosine loading are computed by using NEM, FGM, LAM and AAM. The lumped mass of the system is taken as 1kg and the stiffness is assumed to be $4\pi^2/25$N/m. As a result, the period of the system is found to be 5sec. The system analyzed is assumed to be linear elastic so that the difficulty caused by linearization errors can be avoided. The use of the four methods is intended to study the capability of each method in capturing dynamic loading.

9.1 Separation of Transient Response and Steady-State Response

The system is subjected to a linear polynomial loading of $f(t) = t/t_d$, a sine loading of $f(t) = \sin(2\pi t/t_d)$ and a cosine loading of $f(t) = \cos(2\pi t/t_d)$, where the unit for these loadings is N. It is worth noting that the response to any one of the three dynamic loadings is obtained from the following sequence so that the transient response and steady-state response can be yielded separately. The first step is to obtain the numerical solution by conducting the step-by-step integration with the specified initial conditions so that the transient responses in Eq. (7) can be eliminated. As an example, the initial conditions of $d_0 = a/k - 2c/kp\Omega^2$ and $v_0 = b/kt_d$ must be adopted for the system subject to a polynomial loading. The next step is to compute the response with zero initial conditions so that the total response can be achieved. As a result, the difference in the displacement response between the two numerical solutions gives the transient response.

Numerical results for the linear polynomial loading of are plotted in Fig. 9 for the transient response. Meanwhile, the numerical solutions for the sine loading are plotted in Figs. 10 and 11 and those shown in Figs. 12 and 13 are the results for the cosine loading. The loading duration t_d is taken to be 5sec for each loading case. The vibration period of the sine loading and cosine loading is chosen to be t_d = 2sec and the loading duration is chosen to be 10sec.

9.2 Response to Linear Polynomial Loading

The time steps of Δt = 0.5, 0.25 and 0.125sec, which correspond to p = 10, 20 and 40, are used for the solutions of the responses to the linear polynomial loading. Since the value of $\Delta t/T = \Delta t/t_d = 1/p$ is found, there is almost no period distortion for using Δt = 0.125 and 0.25sec and the use of Δt = 0.5sec will only lead to a slight period distortion. This is manifested from Fig. 9. In this figure, amplitude distortion is not very significant for the four methods and it seems to be less significant than period distortion in each plot, especially for the numerical results obtained from Δt = 0.5sec. These results are consistent with the discretization error amplification factors shown in Fig. 4 and the asymptotic constants shown in the second column of Table 2. For brevity, the steady-state responses to the linear polynomial loading for using the four methods are not presented herein since they are exactly obtained and are consistent with the analytical results. Period distortion is manifested from Fig. 9, where NEM leads to period shrinkage while period elongation is found for the other three methods. FGM shows the least period distortion among the four methods since it is a third-order accurate method while the rest methods are second-order accurate. This example in addition to the discretization error amplification factors reveals that the four methods will lead to roughly the same amplitude distortion for the transient response to linear polynomial loading while the steady-state response is exactly obtained.

https://doi.org/10.1017/jmech.2013.68 Published online by Cambridge University Press

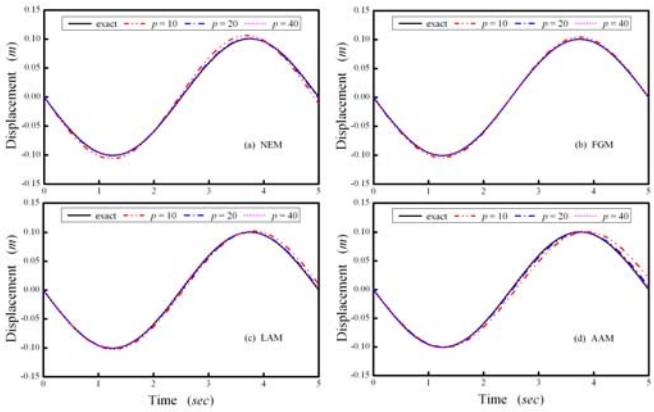


Fig. 9 Comparisons of transient responses to linear polynomial loading

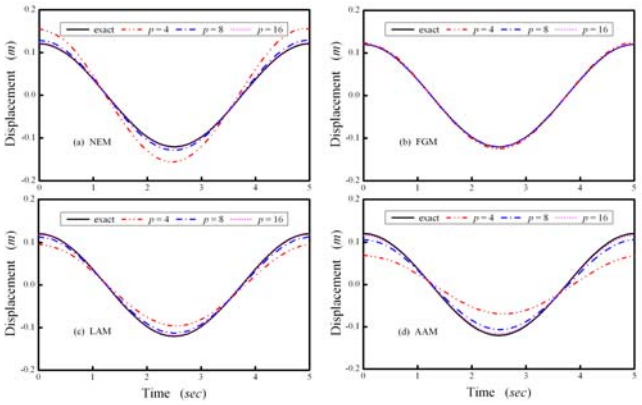


Fig. 12 Comparisons of transient responses to cosine loading

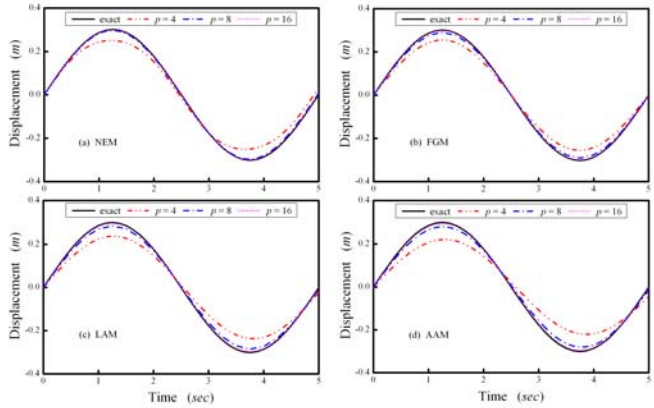


Fig. 10 Comparisons of transient responses to sine loading

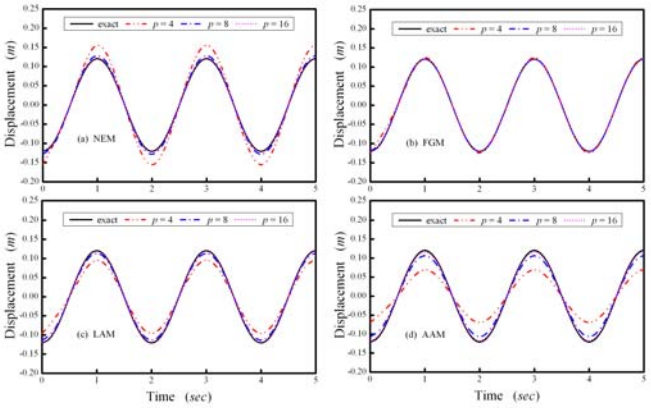


Fig. 13 Comparisons of steady-state responses to cosine loading

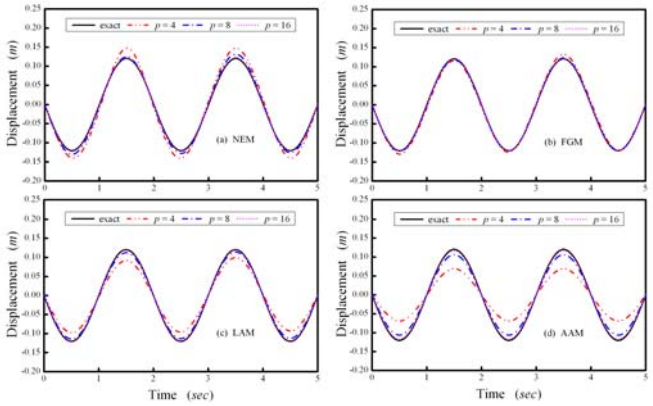


Fig. 11 Comparisons of steady-state responses to sine loading

9.3 Response to Sine and Cosine Loadings

In this example, the responses to the sine loading $f(t) = \sin(2\pi t/t_d)$ and the cosine loading $f(t) = \cos(2\pi t/t_d)$ are obtained from using the four methods. The value of t_d is taken to be 2sec and the time steps of $\Delta t = 0.5$, 0.25 and 0.125sec, which correspond to $p = 4$, 8 and 16, are used to compute the responses to the sine and cosine loadings. Apparently, these time steps will lead to insignificant period distortion since the period of the structural system is 5sec. In each plot of Fig. 10, it seems that the use of $p = 4$ results in too much amplitude distortion while that of $p = 8$ provides an acceptable solution and $p = 16$ leads to a very accurate solution. Amplitude decay is found in each plot of Fig. 10 and the amount of amplitude decay is decreased with the decrease of the time step. In addition, the amount of amplitude distortion is roughly the same for the four methods. These phenomena are in good agreement with the analytical predictions shown in Fig. 5 and the third column of Table 2, where the asymptotic constant of the transient response to sine loading is 1 for the four methods. In Fig. 11, the results obtained from NEM and FGM show amplitude growth for the steady-state response to sine loading while those obtained from LAM and AAM display amplitude decay. Similarly, the amount of amplitude distortion decreases with the decrease of the time step. Meanwhile, the amount of amplitude distortion from the smallest to the largest for the four methods is in the order of FGM, LAM, NEM and AAM. These phenomena are highly consistent with the analytical results shown in Fig. 6 and the third column of Table 2, where the asymptotic constant of the steady-state response to the sine loading is 0, 1, −1 and 2 corresponding to FGM, LAM, NEM and AAM.

In general, the phenomena found in Figs. 12 and 13 for both the transient and steady-state responses to cosine loading are similar to those found in Fig. 11 for the

https://doi.org/10.1017/jmech.2013.68 Published online by Cambridge University Press

steady-state responses to sine loading. This is consistent with the analytical results shown in Eqs. (3) and (7), where amplitude distortion in the steady-state response and the transient response for the cosine loading is exactly the same as that in the steady-state response for the sine loading.

As a summary of this study of the response to harmonic loading, it seems that the use of the four methods with $p = 8$ will give an acceptable response. However, a smaller time step may be recommended for AAM since it leads to more amplitude distortion when compared to the other three methods. This is because that it has the largest asymptotic constant 2 among the four methods for the steady-state response to sine loading, and the transient response and the steady-state response to cosine loading.

10. CONCLUSIONS

A technique to evaluate the capability to capture a specific dynamic loading for an integration method is developed herein. In fact, the asymptotic constant of the discretization error amplification factor for cosine loading is a good indicator for an integration method in capturing a dynamic loading. This study reveals that asymptotic constants of the discretization error amplification factor for both the transient and steady-state responses to cosine loading is found to be $12(\beta - 1/12)$ for the subfamily of Newmark method with $\gamma = 1/2$. This asymptotic constant is generally larger than those of the other dynamic loadings and thus it is very indicative for a specific integration method although many dynamic loading types might be encountered in the step-by-step integration. It is also very important to find that although the subfamily of Newmark method with $\gamma = 1/2$ generally has the second-order accuracy in period distortion, each member shows different capability to capture dynamic loading. As a result, it is needed to evaluate the capability to capture dynamic loading in developing a novel step-by-step integration method.

ACKNOWLEDGMENTS

The author gratefully acknowledges financial support for this study provided by the National Science Council, Taiwan, Republic of China, under Grant No. NSC-96-2221-E-027-030.

REFERENCES

1. Newmark, N. M., "A Method of Computation for Structural Dynamics," *Journal of Engineering Mechanics Division*, ASCE, **85**, pp. 67–94 (1959).
2. Hilber, H. M., Hughes, T. J. R. and Taylor, R. L., "Improved Numerical Dissipation for Time Integration Algorithms in Structural Dynamics," *Earthquake Engineering and Structural Dynamics*, **5**, pp. 283–292 (1977).
3. Chang, S. Y., "Improved Explicit Method for Structural Dynamics," *Journal of Engineering Mechanics*, ASCE, **133**, pp. 748–760 (2007).
4. Chang, S. Y., "An Explicit Method with Improved Stability Property," *International Journal for Numerical Method in Engineering*, **77**, pp. 1100–1120 (2009).
5. Chang, S. Y., "A New Family of Explicit Method for Structural Dynamics," *Computers & Structures*, **88**, pp. 755–772 (2010).
6. Belytschko, T. and Hughes, T. J. R., *Computational Methods for Transient Analysis*, Elsevier Science Publishers B.V., North-Holland (1983).
7. Chang, S. Y., "Accuracy of Time History Analysis of Impulses," *Journal of Structural Engineering*, ASCE, **129**, pp. 357–372 (2003).
8. Chopra, A. N., *Dynamics of Structures*, Prentice Hall, Inc., International Editions (1997).
9. Bathe, K. J., *Finite Element Procedures*, Prentice Hall, Inc., International Editions (1996).
10. Strang, G., *Linear Algebra and its Applications*, Harcourt Brace Jovanovich, San Diego (1986).

(Manuscript received April 3, 2012,
accepted for publication August 5, 2013.)

https://doi.org/10.1017/jmech.2013.68 Published online by Cambridge University Press